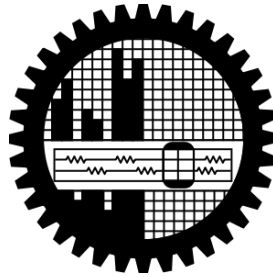


PERFORMANCE OF WATER COOLED MINICHANNEL HEAT SINK WITH CROSS FLOW

By

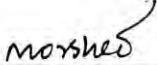




MASTER OF SCIENCE IN MECHANICAL ENGINEERING



**Department of Mechanical Engineering
Bangladesh University Of Engineering And Technology**

This thesis titled “Performance of Water Cooled Minichannel Heat Sink with Cross Flow” submitted by **Md. Fazlul Bari**, Roll No: **0413102131**, Session: April/2013 has been accepted as satisfactory in partial fulfillment of the requirement for the degree of **Master of Science in Mechanical Engineering** on 1/11/2017.

BOARD OF EXAMINERS

1. 
Dr. A K M Monjur Morshed
Associate Professor
Department of ME, BUET, Dhaka
Chairman
(Supervisor)
2. 
Head
Department of ME, BUET, Dhaka
Member
3. 
Dr. M. A. Rashid Saikar
Professor
Department of ME, BUET, Dhaka
Member
4. 
Dr. Mohammad Nasim Hasan
Associate Professor
Department of ME, BUET, Dhaka
Member
5. 
Prof. Dr. Md. AbdurRazzaqAkhanda
6/4-A, Iqbal Road
Mohammadpur, Dhaka
Member
(External)

CANDIDATE'S DECLARATION

It is hereby declared that this thesis or any part of it has not been submitted elsewhere for the award of any degree or diploma.

Md. Fazlul Bari

November 2017

Md. Fazlul Bari

ACKNOWLEDGEMENTS

First of all I would like to express our gratitude to Allah for bestowing us with the ability to complete this work properly.

Then I like to acknowledge our earnest grateful to our esteemed supervisor Dr. A. K. M. Monjur Morshed whose continuous supervision has enabled me to complete this whole work. Along the way whenever I encountered any hurdle he gave me important instructions that made it possible for me to find a way around. He gave me significant insights into my work that went a long way in accomplishing this task. Without his careful supervision, it would have been impossible for me to pull this task off in time with due diligence.

I would also like to express our thankfulness to our family members, especially my parents without whose support and encouragement the whole endeavor would not have been as streamlined as it has been.

ABSTRACT

Minichannels embedded in solid matrix has already been proven as a very efficient way of electronic cooling. Traditional minichannel heat sink consists of a single layer of parallel channels fabricated in silicon or copper substrate. Although the minichannel heat sink can achieve very high heat flux, its pumping requirement for circulating liquid through the channel increases very sharply as the flow velocity increases. Besides, there exists a very sharp temperature rise along the length of the mini channel heat sink. In many cases, the hydrodynamic developing length covers a large portion of the channel and the thermal entrance length is more than the channel length. As the hydrodynamic and thermal boundary layer grows, heat transfer coefficient reduces due to the thickening of the boundary layer. By breaking the boundary layer along the flow length, thermal boundary layer can be redeveloped and thus the benefit of the higher heat transfer coefficient of the entry region can be achieved. Thus, by dividing the flow channel into several zones with the cross channel, heat removal capacity of the heat sink can be increased and at the same time pumping requirements can be reduced.

The hydrodynamic and thermal characteristics of the minichannel with cross connection has been studied experimentally and numerically. The effect of the cross channel on the thermal performance of the mini channel heat sink has been investigated. A maximum of 18% heat transfer enhancement has been achieved with the cross connection compared with the straight minichannel heat sink. Based on the experimental results, a numerical investigation by using FLUENT has been performed to improve understanding of the fundamental mechanisms involved with the cross channel. Some parametric studies have also been performed with this numerical model to optimize the design parameters of the heat sink with cross connection.

Contents

ABSTRACT	5
1. CHAPTER -1	1
INTRODUCTION.....	1
1.1. Motivation for the Study	1
1.2. Research Objective	3
1.3. Outline of the dissertation	3
2. CHAPTER -2	4
LITERATURE REVIEW	4
2.1. Micro channel and Mini Channel Heat Sink	4
2.2. Heat Transfer Enhancement Techniques Of Small Size Channel	7
2.2.1. ACTIVE TECHNIQUE.....	7
2.2.1.1 Vibration	7
2.2.1.2 Flow pulsation	8
2.2.1.3 Electrostatic Fields.....	8
2.2.1.4 Synthetic Jet	9
2.2.1.5 Jet impingement.....	10
2.2.2. PASSIVE TECHNIQUE	10
2.2.2.1 Surface Roughness	10
2.2.2.2 Micro Pillar and Other Flow Obstruction.....	11
2.2.2.3 Redeveloping Flow.....	12
2.2.2.4 Using nanofluid	13
2.2.2.5 Channel curvature.....	14
2.2.2.6 Twisted microchannel	15
2.3. LIMITATIONS OF MICRO/ MINI CHANNEL HEAT SINK	15
2.4. SUMMARY	16
3. CHAPTER -3	17
EXPERIMENTAL SETUP	17
3.1. Water Flow Loop	17
3.2. Test Section	18
3.3. Data Acquisition	20
3.4. Experimental Methods	21

3.5.	DATA REDUCTION.....	22
3.6.	Experimental Uncertainties.....	23
4.	CHAPTER 4	24
	NUMERICAL MODEL AND SIMULATION METHODS	24
4.1.	Schematics of the Model.....	24
4.2.	Mathematical Formulation.....	26
4.3.	Boundary Conditions	27
4.3.1.	Hydraulic Boundary Conditions.....	27
4.3.2.	Thermal Boundary Conditions	27
4.3.3.	Coolant and Material property of the heat sink	28
4.4.	Simulation setup.....	29
4.5.	Mesh Independence Test	29
5.	CHAPTER 5	30
	RESULTS AND DISCUSSION.....	30
5.1.	RESULTS OF THE EXPERIMENTAL STUDY.....	30
5.1.1.	Benchmark Test.....	30
5.1.2.	Performance of the heat sink.....	32
5.2.	RESULTS OF THE NUMERICAL STUDY	37
5.2.1.	Model Validation	37
5.2.2.	Effect of the Channel Enlargement	38
	39
5.3.	Effect of the flow velocity.....	39
5.3.1.	Effect of the cross connection.....	40
6.	CHAPTER -6	43
6.1.	Conclusions.....	43
6.2.	Future Recommendations	44
7.	REFERENCES	45

LIST OF FIGURES

Figure 2.1: Piezoelectric enhanced channel [9].....	8
Figure 2.2: Electrostatic forces in a minichannel (Steinke and Kandlikar, 2004).	9
Figure 2.3: Synthetic jet actuated in a micro channel [13].....	9
Figure 2.4: Jet impingement cooling in a mini channel [14].....	10
Figure 2.5: CuNWs decorated micro channel [15].....	11
Figure 2.6: Microfin inside the microchannel [16].....	12
Figure 2.7: Microchannel with redeveloping flow [17]	12
Figure 2.8: TEM image of the nano particles suspended in the base fluid [22]	14
Figure 2.9: Curved micro channel [23]	14
Figure 2.10: three-dimensional twisted micro channel, bondar and battaglia [25]	15
Figure 3.1: Water flow loop	17
Figure 3.2: (a) Test Module; (b) Test module-1; (c) test module-2 (with cross channel)	19
Figure 3.3: Test section used for the experiment and Cu block with the straight minichannel ...	20
Figure 3.4: Thermocouple display and selector switch, variac, gear pump and the cartridge heater used in the experiment.....	21
Figure 4.1: Computational domain (a) Simple micro-channel (b) Cross section of computational domain (c) Transverse channels	25
Figure 5.1: Nusselt number as a function Reynolds number.....	31
Figure 5.2: Copper heat sink temperature at different thermocouple location and different Reynolds no.....	33
Figure 5.3: Comparison of the Surface temperature between the channel having cross connection and does not have any cross connection.....	34
Figure 5.4: Comparison of the Surface temperature for different input power.	34
Figure 5.5: Comparison of the average heat transfer coefficient for different input power.	35

Figure 5.6: Comparison of the h_x as a function of x^* for both the straight channel heat sink and heat sink with cross connection.....	35
Figure 5.7: Comparison of the Nu_{avg} as a function of Re for both the straight channel heat sink and heat sink with cross connection	36
Figure 5.8: Comparison of the experimental results with that of the simulation for straight mini channel.....	37
Figure 5.9: Comparison of the experimental results with that of the simulation for straight mini channel.....	38
Figure 5.10: plot of temperature contour for simple micro-channel computational domain for $Re=98$	39
Figure 5.11: Effect of the velocity on the temperature distribution of the channel (a) heat sink with the cross channel; (b) heat sink without cross channel.....	39
Figure 5.12: Velocity contour of the heat sink (a) channel without cross connection; (b) channel with cross connection; (c) boundary layer redevelopment around the cross connection	40
Figure 5.13: Average Nusselt number as a function of the Reynolds number	41
Figure 5.14: Temperature contour of heat sink at the plane at $y=0$ for 76 volt and $Q=500\text{ml/min}$ (a) simple micro-channel (b) transverse micro-channel.....	41
Figure 5.15: Overall thermal resistance vs pumping power	42

LIST OF TABLES

Table 2.1: Classification of channel	5
Table 3.1: uncertainty associated with the experiment.....	23
Table 4.1: Key dimensions of the model.....	28
Table 4.2: The Material property used in the simulation	28

LIST OF SYMBOLS, SUBSCRIPTS AND ABBREVIATIONS

1. Symbols

N_u	Nusselt Number
P_u	Prandtl number
k_f	Fluid thermal conductivity
D_h	hydraulic diameter.
Δp	pressure Different
Q	Volumetric flow rate
ρ	density
C_p	specific heat
T_m	Fluid means temperature
T_s	Surface temperature
V	voltage
I	current
Q_{in}	Input power
$T_{i,s}$	surface temperature
K_{cu}	Thermal conductivity of the copper.
PP	pumping power
L_{entry}	Entry length
h	heat transfer coefficient
z/Z	Dimensionless Channel Length .
R_t	Overall Thermal Resistance
X^*	Dimensionless distance

q	Rate of heat flux
x	Channel Length

2. Subscripts

ref	Reference
U	Upper wall
L	Lower wall

CHAPTER -1

INTRODUCTION

1.1.MOTIVATION FOR THE STUDY

The heat removal issue is very important in many engineering applications and it becomes critical to the advancement of the modern micro-electronics industry. Efficient removal of ever increasing heat flux of the advanced micro electronics has become a major challenging issue for the thermal engineers. Heat flux of some electronic devices has already touched 100 w/cm^2 [1], which once thought to be too high for the electronic devices. The trends to miniaturize the electronic devices and to increase the packaging density are increasing very fast specially for the defense equipment related electronics, *i.e.* radar, laser weapons, etc. where 1000 w/cm^2 becomes a reasonable heat removal target [2], which exceeds the capability of the most advanced cooling technology. To keep pace with the current growth trend of microelectronics devices, efficient and reliable thermal management solution is necessary which is capable of extracting gigantic heat load from a nanometer size chip with surface temperature less than a prescribed value.

Generally, thermal management of electronic system consists of two levels to diffuse heat from the device to the ambient. The first level is the package-level, in which the heat generated from the integrated circuit or die is rejected to a substrate through appropriate packaging techniques. In the second-level, heat is removed from the substrate surface to the ambient.

Typically, the total thermal resistance from the device to ambient can be expressed as:

$$R_{tot} = DF * R_{package} + R_{TIM} + R_{sink} \dots \dots \dots (1.1)$$

Where, R_{tot} , $R_{package}$, R_{TIM} , and R_{sink} are the thermal resistance of package, thermal interface material and heat sink or similar device, respectively. Density factor (DF), accounts for the non-uniformity of heat generation [3].

For performance and reliability, the junction temperature of the die has to be within 90–110°C range [4]. The thermal resistance between the package and heat sink, R_{TIM} (Interfacial Thermal Resistance), is typically a very small portion compared to the total thermal resistance. Therefore, thermal designers are left with two choices: (i) decrease the thermal resistance of packaging ($R_{package}$) and (ii) decrease the thermal resistance of the heat sink (R_{sink}). Since the thermal resistance near the die, $R_{package}$ gets multiplied by the DF, any reduction in the package resistance results in a larger reduction of R_{tot} . One of the main focus of the next-generation electronics cooling is developing efficient cooling solutions near the package. On the other side, reduction of R_{sink} is even more important to reduce R_{tot} , since the thermal resistance of heat sink or similar device is dominant in many applications. In this work, the research mainly focuses on developing advanced cooling strategies to reduce R_{sink} .

Among the three modes of heat transfer, conduction is dominant at the package-level; and at temperatures less than 110°C radiation is comparable to natural convection heat transfer. Therefore, forced convection heat transfer is the key mechanism to improve R_{sink} . Many advanced cooling schemes have been studied in recent years to meet this demand; *i.e.* thermo-electric cooling, heat pipe, piezo fan, immersion cooling, jet impingement cooling, thermoionic and thermo-tunneling cooling, etc. [5]. Among different cooling technologies, micro thermo-fluidic based liquid cooling is considered one of the most effective solutions [6].

In micro thermo-fluidic based liquid cooling technology, water or other liquid passes through small passages carrying heat. As the flow passage dimension reduces, its surface area to volume ratio increases, causing an increase in heat transfer rate. However, this enhanced thermal performance is accompanied by an increased pressure drop penalty. The smaller dimension channel increases volumetric heat transfer density, which requires advanced manufacturing techniques and more complex manifold designs. An optimal balance for each application leads to different channel dimensions.

In this work, a novel cooling scheme based on passive enhancement technique adopted in the mini size channel has been investigated. Mini-size channel introduces less complexity

in manufacturing and manifold design than the micro size channel; however the passive enhancement technique adopted inside the mini channel will lead to better thermal performance compared to the plain minichannel.

1.2. RESEARCH OBJECTIVE

The proposed research is an experimental investigation followed by a numerical analysis focused on enhancing the heat transfer performance of the minichannel heat sink. The key objectives of this present research are:

- To investigate the thermal performance a conventional minichannel heat sink.
- To investigate the thermal performance of the mini channel heat sink with the proposed passive enhancement technique.
- To develop a numerical model of the proposed heat sink.
- To optimize the proposed concept with the numerical analysis.

1.3. OUTLINE OF THE DISSERTATION

The dissertation is organized as follows. Literature review related to the present work has been presented in chapter-2. Chapter-3 describes the experimental methods and procedure for this study. Chapter-4 includes the numerical modeling of the experimental work. Chapter-5 presents the results and a discussion of the experimental investigation followed by the results of the numerical simulation. A short summary of the main conclusions and recommendations for the future work is presented in Chapter-6.

CHAPTER -2

LITERATURE REVIEW

With the advances of machining technology, the development of miniaturized devices has been rapidly increasing, especially in the electronic engineering, medical engineering and other fields. Due to the small dimension and high heat flux of the electronic devices, air cooling has become inadequate to meet the thermal demand of the next generation electronics. Water cooled mini and micro channel has been widely studied by the researchers as a solution to the advanced electronic cooling. In this chapter a comprehensive review has been presented in micro and mini channel cooling and different enhancement technique that has been studied by previous researchers.

2.1. MICRO CHANNEL AND MINI CHANNEL HEAT SINK

Among various key and promising cooling strategies, micro and mini channel heat sinks have been proven to be a high-performance cooling technique that is capable of dissipating high heat fluxes from electronic devices. It is usually made from a high thermal conductive solid substrate such as silicon or copper with parallel micro/mini channels fabricated into the substrate. The channels have characteristic dimensions ranging from 10 μm to upward. Channel size has a profound effect on different processes and acting forces, resulting in heat transfer characteristics different than that of the classical channel. Considering the number of processes and parameters that govern transitions from regular to microscale phenomena, a simple dimensional classification is generally adopted in literature [2] as presented in the table below.

Table 2.1: Classification of channel

Sl. No.	Parameters	Size
1.	Conventional channel	$> 3 \text{ mm}$
2.	Minichannel	$3 \text{ mm} \geq D > 200 \text{ }\mu\text{m}$
3.	Microchannel	$200 \text{ }\mu\text{m} \geq D > 10 \text{ }\mu\text{m}$
4.	Transitional Microchannel	$10 \text{ }\mu\text{m} \geq D > 1 \text{ }\mu\text{m}$
5.	Transitional Nanochannel	$1 \text{ }\mu\text{m} \geq D > 0.1 \text{ }\mu\text{m}$
6.	Nanochannel	$0.1 \text{ }\mu\text{m} \geq D$

The shape of the channel cross-section can be rectangular, triangular, circular or trapezoidal. A liquid such as water, electronics coolant or refrigerant is pumped into the channels. The heat generated by the electronic devices is transferred to the substrate and absorbed by the cooling fluid that flows through the channels. Depending on the flow and heat transfer conditions, the cooling fluid can be in single-phase state or experiences liquid-vapor phase change inside the channels, which classifies micro/ mini channel heat sinks into single-phase or two-phase.

The most well-known work, by Tuckerman and Pease [7], is often considered to be the pioneering study of introducing the concept of micro-channels for electronics cooling. They employed the direct circulation of water in micro-channels fabricated on a 1 cm x 1 cm silicon chip. Their heat sink can dissipate heat fluxes as high as 790 W/cm^2 with a maximum substrate temperature to inlet water temperature difference of 71°C . However, the pressure drop is very high, which is around 214 kPa.

The idea of using smaller channels to improve thermal performance of the heat sink has been fairly simple. For convective heat transfer in channels having a hydraulic diameter of D_h , the heat transfer coefficient is calculated as:

$$h = \frac{k_f Nu_{D_h}}{D_h} \quad 2.1$$

Where, k_f is fluid thermal conductivity, and Nu_{D_h} is the nusselt number for the flow condition. For example, for laminar fully developed flow in a circular passage with constant heat flux, $Nu_{D_h} = 4.36$. It can be seen that heat transfer coefficient is generally increased with decreasing channel size. The passage size should be made as small as possible to enhance the heat transfer rate. Whereas, reducing the passage size will increase the pressure drop penalty. In other arguments, the heat transfer enhancement is at the expense of higher pressure loss. The pressure loss is given by:

$$\Delta p = \frac{1}{2} \rho U^2 f \frac{L}{D_h} \quad 2.2$$

Where, ρ is the fluid density, U is the fluid velocity, L is the channel length, and f is the friction factor. For fully developed laminar flow in a square channel, the friction factor is $f = 64/Re_{D_h}$. Here, Re_{D_h} is the Reynolds number (UD_h/ν), where ν is the fluid kinematic viscosity. Therefore, it can be approximately conclude that $\Delta p \propto \frac{1}{D_h^2}$, *i.e.*, reducing the channel size will increase the pressure drop quickly.

It is desirable to have the pressure drop in micro-channels be at the level of 35 kPa (5 psi) [8]. This number is based on the pressure available from the compact and reliable pumps reduced by the pressure drop in other system component such as heat exchangers, connectors, filters, and distribution piping. Generally, for single-phase channel flow, depending on the channel size and flow rate, the flow regime can be laminar or turbulent, and the flow condition can be developing flow or fully developed flow. However, with a pressure drop less than 35 kPa, the channel flow is most likely fallen in the laminar regime, either developing or fully developed. As it is already known, heat transfer in laminar flow is much lower compared to the turbulent flow.

The primary focus of single-phase micro and minichannel research is on predicting and validating its hydraulic and thermal performances. Much less attention has been directed for developing effective thermal enhancement strategies for micro and minichannels. The

single-phase heat transfer enhancement techniques have been well established for conventional channels and compact heat exchangers. The major techniques include flow transition, breakup of boundary layer, entrance region modification, introduction of vibration inside the channel, application of electric fields, swirl flow, secondary flow and mixing of the fluid [4]. Some of these techniques can be extended into micro and minichannel applications. Different techniques adopted for micro and mini channel heat transfer enhancement are presented in the following section.

2.2. HEAT TRANSFER ENHANCEMENT TECHNIQUES OF SMALL SIZE CHANNEL

Two types of techniques are available for the heat transfer enhancement of micro and mini channel:

- i. Active technique
- ii. Passive technique

Some example of active and passive enhancement techniques that have been adopted previously has been presented in the following section:

2.2.1. ACTIVE TECHNIQUE

Active technique involves external power input for heat transfer enhancement; *i.e.* induced pulsation flow, use of a magnetic field, mechanical aids to enhance the mixing inside the channel, surface vibration, fluid vibration, electrostatic fields, suction or injection of fluid inside the channel and jet impingement [9]. Some examples of active technique are presented in the following section:

2.2.1.1 Vibration

Vibration in the fluid or at the surface of the fluid layer is an active method that has been used in conventional channels. Although vibrating the tube is not a convenient option for the mini or micro channel, However the technique can be adopted easily with the piezoelectric actuated micro fin. As the fluid moves over the micro fins, a vibration is induced that breaks up the boundary layer causing heat transfer enhancement [10].

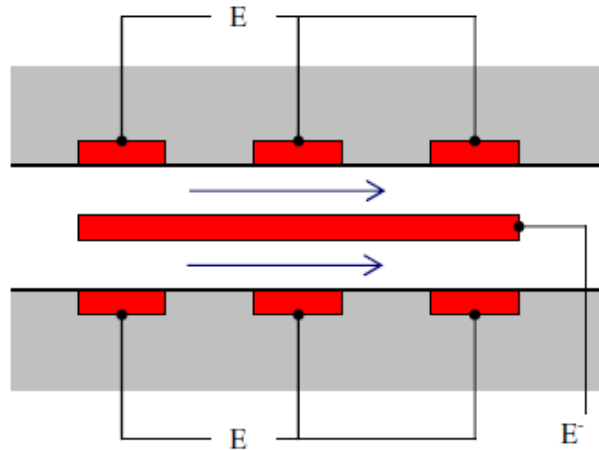


Figure 2.2: Electrostatic forces in a minichannel (Steinke and Kandlikar, 2004).

2.2.1.4 Synthetic Jet

Synthetic jet provides periodic disturbances in the flow path. Synthetic jet has been studied for microchannel flow by Ruixian *et. al.*[12]. Periodic disturbance is generated when the synthetic jet interacts with the microchannel flow. Heat transfer performance is enhanced as local turbulence is generated and propagated downstream the microchannel. It shows that the thermal effects of the synthetic jet are very profound and up to 42% heat transfer enhancement has been reported.

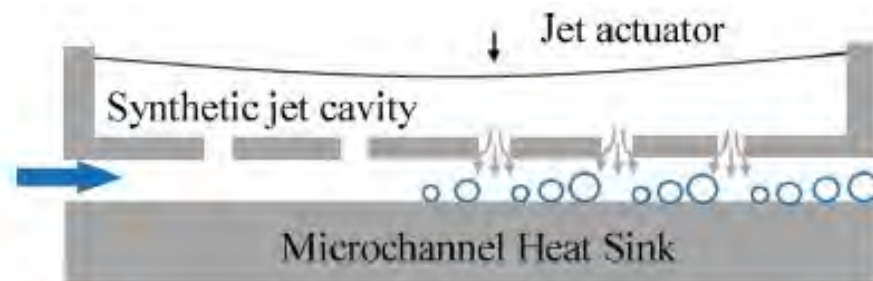


Figure 2.3: Synthetic jet actuated in a micro channel [13]

2.2.1.5 Jet impingement

Cross flow jet disturbs the boundary layer of the channel and enhances heat transfer inside the channel. Due to the cross flow from the jet, boundary layer of the channel breaks up which also introduces turbulence resulting in enhanced heat transfer [14].

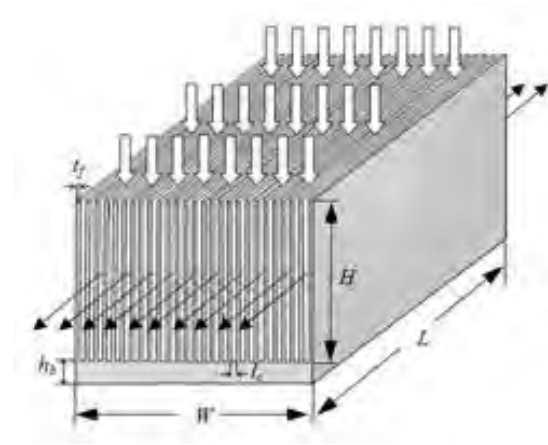


Figure 2.4: Jet impingement cooling in a mini channel [14]

All the active techniques have a more profound effect on the heat transfer enhancement. However, it increases the complexity of the device and also increases the operating cost.

2.2.2. PASSIVE TECHNIQUE

The passive enhancement technique does not require any external power source resulting in less complexity in application, thus they are more desirable. Some of the basic techniques used for the passive enhancement include: flow disruption, secondary flow, surface treatment, and entrance effect. Several of these techniques already have been implemented in micro and mini channels.

2.2.2.1 Surface Roughness

One of the passive techniques to improve the thermal performance of micro or mini channel is to alter the surface morphology of the heated surface. This method reduces thermal boundary layer thickness and also aids in early transition into turbulent flow. The conventional way to alter the surface is to increase the roughness of the surface. Kandlikar studied the effect of surface roughness in a minichannel flow [9]. Recently several micro and nanoscale surface modification techniques have been applied for microchannel. Although nanoscale surface modification is more effective in two phase

flow, However they are also effective in single phase flow. CuNWs developed inside a channel can increase the heat transfer rate upto 24% compared to the plain surface [15].

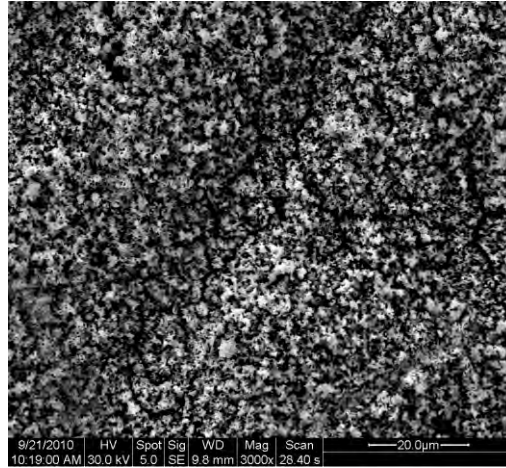


Figure 2.5: CuNWs decorated micro channel [15]

2.2.2.2 Micro Pillar and Other Flow Obstruction

With the aid of the advanced manufacturing technology, it is now possible to construct micro and nano fin inside the micro and mini channel. Micro and nano fin inside the micro channel promote mixing of the cold and hot fluid resulting in enhanced heat transfer. Similar to the micro fin micro grooves inside the channel also can promote the mixing and breaking the thermal boundary layer causing heat transfer enhancement. Very high heat fluxes can be dissipated at low wall temperature rise using a microscale pin fin inside the channel. However, the heat transfer and pressure drop correlations are currently not sufficiently developed, but the results strongly suggest that pin fin heat sinks deserve adequate research attention [16].

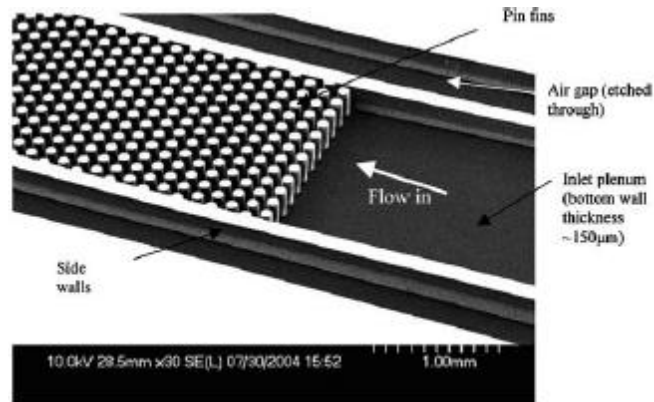


Figure 2.6: Microfin inside the microchannel [16]

2.2.2.3 Redeveloping Flow

In General, length of a high heat flux chip is several times of the thermal developing length. Heat transfer rate is higher for the thermal developing zone compared to the developed zone. If the flow length of the microchannel can be separated into several independent zones that ensure the thermal developing flow in each independent zone, and thus the overall heat transfer can be enhanced. Xu *et. al.* studied the microchannel heat transfer enhancement using thermal boundary layer redeveloping concept and concluded this new microchannel heat sink can significantly reduce the pressure drops while enhancing heat transfer [17].

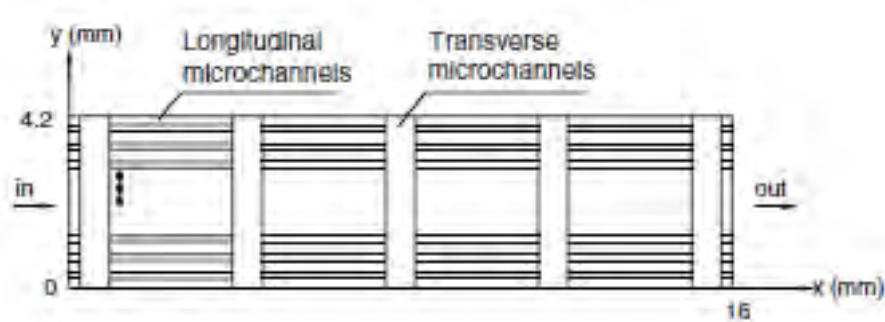


Figure 2.7: Microchannel with redeveloping flow [17]

2.2.2.4 Using nanofluid

In a thermal system, convective heat transfer rate can be enhanced either by changing flow geometry, boundary conditions, or by improving thermo-physical properties, for example, enhancing fluid thermal conductivity. Suspending small solid particles in a fluid represents an innovative way to improve its thermal conductivity of the fluid. Since the thermal conductivity of solid is higher than that of fluids, the suspended particles are expected to be able to increase the thermal conductivity of the flowing fluid and heat transfer performance. Metallic, non-metallic and polymeric particles are used to form slurries by adding into fluids. Owing to the fact that size of the particles creating different problems such as abrasion and clogging, recent advancements in manufacturing technologies have made the production of particles in nanometer scale possible eliminating those problems. The uniform and stable suspensions are obtained by means of these smaller sized particles, thus providing higher heat transfer enhancements. Several investigations revealed that the thermal conductivity of the nanoparticles suspension could be increased by more than 20% for the case of very low nanoparticles concentrations. In spite of the two phase mixture prevailing in nanofluids, they are easily fluidized and can be nearly considered to behave as a fluid [18] due to the tiny size of solid particles making it possible to treat them as single phase flow. It is assumed that the fluid phase and particles are in thermal equilibrium and moving with the same velocity in a certain condition taking into account the ultra-fine and low volume fraction of the solid particles. The most well-known nanoparticles have been used by many researchers in their experimental works together with the base fluids of water and ethylene glycol. In spite of the different size of the particles and type of base fluids, the enhancement of the thermal conductivity was observed during all the experimental conditions. The first empirical correlations for the determination of Nusselt number for laminar and turbulent flow of a nanofluid inside a tube have been developed by Pak and Cho [19] using the mixture of water and copper, nanoparticles. Masuda [20] reported thermal conductivity enhancement by 30% using water- nanofluid having 13 nm mean diameter particles at 4.3% volume fraction. The heat transfer coefficient in the entrance region and in the fully developed region have been found to be increased by 17% and 27% respectively [21]. However, the main challenge in enhancement of heat transfer using nanofluid is the

deposition of nanoparticle which requires further investigation and development of nanofluid having no deposition issue.

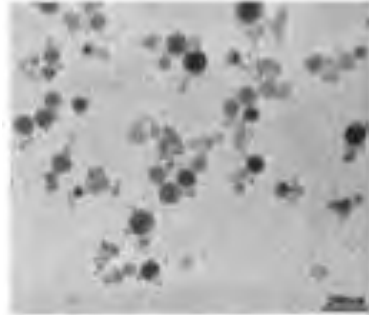


Figure 2.8: TEM image of the nano particles suspended in the base fluid [22]

2.2.2.5 Channel curvature

Several researchers have demonstrated that heat transfer enhancement can be achieved by having a curved flow path [2]. The traditional parabolic velocity profile is skewed due to the additional acceleration forces. This causes the angle between the gradients to decrease and facilitate enhancement. Sturgis and Mudawar [23] demonstrated the heat transfer enhancement in a curved channel. This technique is not really practical in a large sized conventional passage, However it has a good potentiality in micro and mini channel. The radius of curvature can be on the order of a few millimeters to centimeters but considered to be large compared to the channel diameter. The compact nature of the micro channel flow network could allow for a serpentine flow channels to utilize the curvature enhancement.

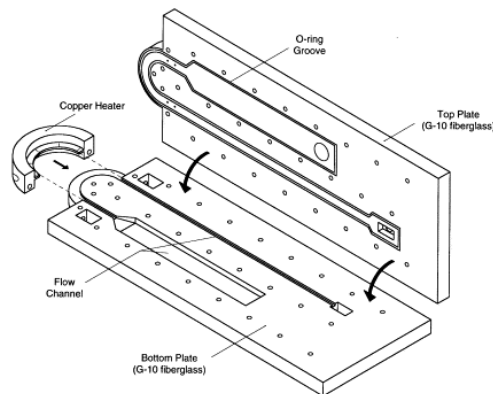


Figure 2.9: Curved micro channel [23]

2.4. SUMMARY

From the works reviewed above, it shows that passive technique is more desirable due to less complexity in applications and it is reliable. The cross connection channel can be used to enhance the heat transfer performance without increasing the pressure drop penalty. However, this strategy has rarely been investigated in mini channel heat transfer augmentation. Besides cross connection doesn't provide the desirable heat transfer enhancement if there is very limited flow in the cross channel. The cross channel strategy that has been previously studied has been modified in this research to increase the cross velocity and the concept has been examined both numerically and experimentally in this study.

CHAPTER -3

EXPERIMENTAL SETUP

The experimental system has been designed and constructed to conduct the experimental studies on the various transport phenomena associated with single-phase flow in the minichannel with the cross flow cooling scheme. Details of the experimental system, including a flow loop, test modules and data acquisition system are presented in this chapter.

3.1. WATER FLOW LOOP

Figure 3.1 shows the experimental setup used in this study. The test loop was an open loop configuration. From an inlet reservoir DI water has been pumped to the test section by a gear pump (ISMATEC® Regol-z digital), which can provide a constant mass flow rate. The pump has been equipped with a digital flow meter which has been calibrated by the bucket and stopwatch method. Two thermocouples have been placed one at the inlet and the other one at the outlet for measuring inlet and outlet temperature of the fluid. Two cartridge heaters have been connected in parallel, powered by a 0-220V variac.

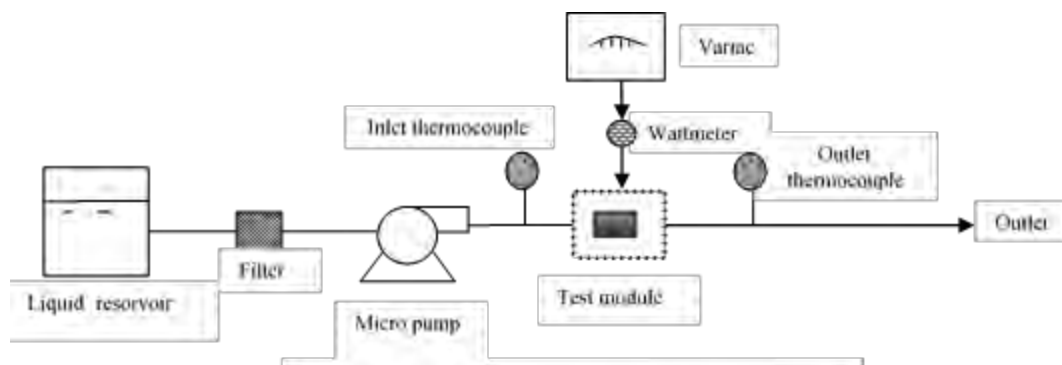


Figure 3.1: Water flow loop

3.2. TEST SECTION

Two test modules have been constructed for the experiment: (i) heat sink with the straight minichannel and (ii) minichannel heat sink with cross connection.

The test modules consist of glass cover plate, Cu test section, housing block, and two cartridge heaters as illustrated in Figure 3.2. For fabrication of the minichannel heat sink a copper block has been selected. The top surface of the copper block was 20 mm wide and 50 mm long. Fourteen rectangular mini slots have been machined on the top surface of the block using an EDM wire cut machine in two portions; seven channel on each side.

The channel dimensions have been 0.5 mm \times 0.5 mm \times 50 mm. Two cartridge heaters of 5.75 mm diameter and 40.5 mm length have been inserted into the bottom portion of the copper block to supply the heat flux. Five 'K' type thermocouples have been inserted up to the half of the width of the channel below the minichannel for measuring local temperature along the channel. Thermal glue has been applied at the interface of the thermocouple and the Cu block.

The central portion of the Nylon-66 plastic housing has been removed to place the copper block. High temperature RTV silicone glue has been applied at the interface between housing and copper block to seal them tightly to avoid any water leakage. The housing contains two plenums: one on the upstream and the other one of the downstream of the mini channel. Inlet and outlet thermocouples have been placed at these two plenums.

A glass plate has been placed on top of the housing by RTV silicon glue and clamped with the housing by 'C' clamp to ensure leak proof assembly.

For the second test module, eighteen transverse channel of length 2 mm, width 0.5 mm and depth 0.5 mm have been machined at the top surface of the copper block at different position of the fourteen longitudinal channels as illustrated in Figure 3.2 (b). The transverse channels have been separated lengthwise by 11 mm. The housing, cartridge heaters have been same as in the mini channel heat sink without transverse channel.

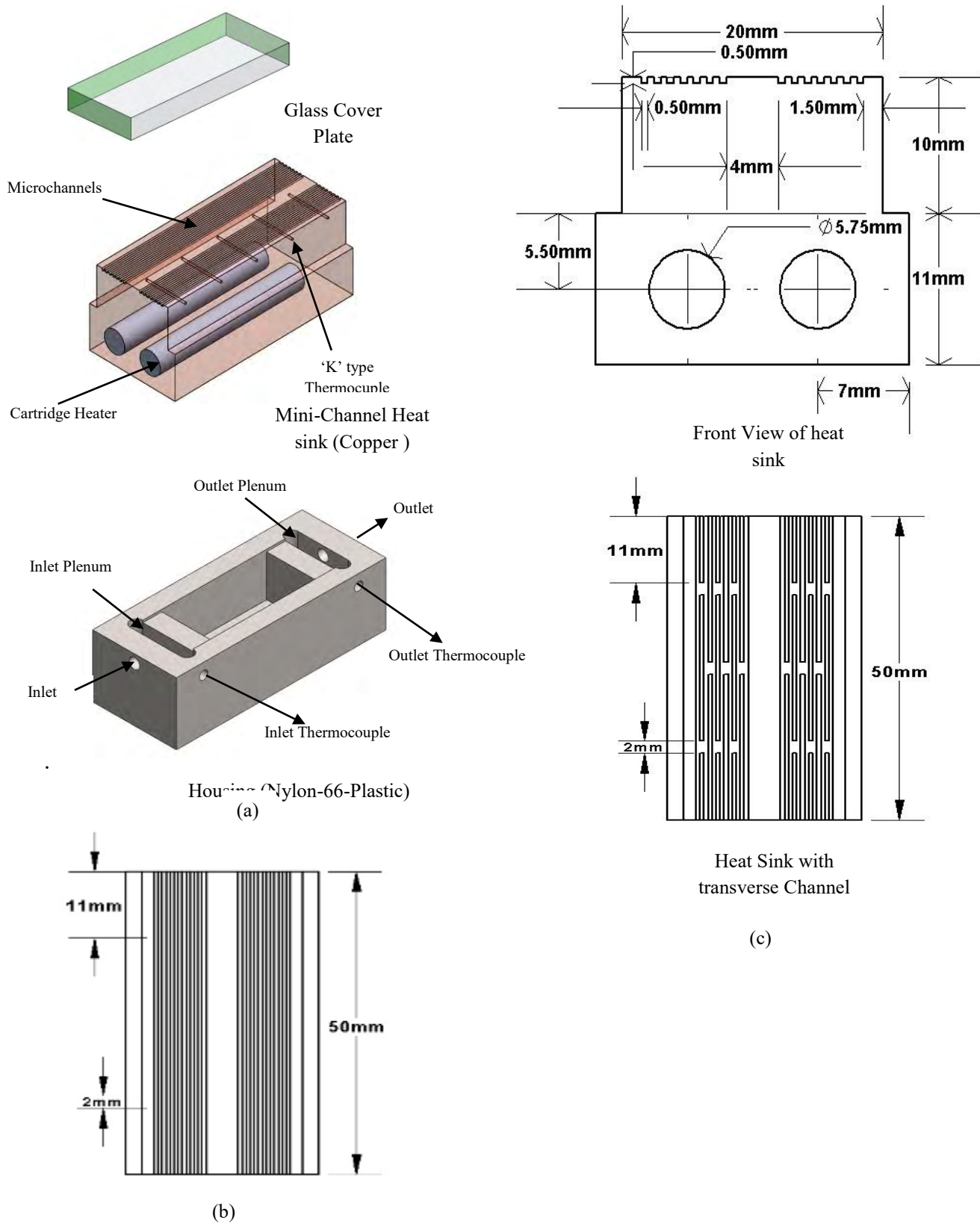


Figure 3.2: (a) Test Module; (b) Test module-1; (c) test module-2 (with cross channel)



Figure 3.4: Thermocouple display and selector switch, variac, gear pump and the cartridge heater used in the experiment

3.4. EXPERIMENTAL METHODS

To perform the experiment, the test section has been assembled and connected in the flow loop; the pump has been set to run at a desired flow rate by adjusting the pump control panel. After the flow rate and inlet temperature have been stabilized, a predetermined level of power has been supplied to the heater from the Variac. Usually it requires 20-30 min for the test section to reach steady state. Steady state is considered to be achieved when the average temperature of the thermocouples remains constant over a ten minutes time interval. About 10 data points each at one minute interval have been collected after the system reached steady state. The readings have been repeated for 3 times with a 5 minute time interval. Once the data recordings are completed, the flow rate has been varied, keeping the power supply constant. DI water has been used as a coolant. The whole experimental procedures have been repeated for two power levels of the cartridge heater.

3.5. DATA REDUCTION

The steady-state sensible heat gain Q by the coolant can be determined from an energy balance:

$$Q = \rho C_p (T_{in} - T_{out}) \dot{Q} \quad (3.1)$$

Where, \dot{Q} is the volumetric flow rate (measured from the pump control panel), density (ρ) and specific heat (C_p) have been obtained using fluid mean temperature (T_m).

$$T_m = (T_{in} + T_{out})/2$$

In this experiment, voltage (V) and current (I) was measured directly from the power supply and input power (Q_{in}) to the cartridge heater was calculated.

$$Q_{in} = V.I \quad (3.2)$$

Depending on the flow rate, 70 ~80 % of the input power is carried by the flowing water. Heat losses from the experimental setup have been calculated by deducing the energy gained by the water from the total electrical power input.

$$Q_{loss} = Q_{in} - \rho C_p (T_{in} - T_{out}) \dot{Q} \quad (3.3)$$

Surface temperatures of the heat sink were estimated from 1D steady state conduction equation coupling with the thermocouple's reading (thermocouples inserted into the copper block).

$$T_{i,s} = T_i - Q.t/K_{cu}.A_t \quad (3.4)$$

Where, $T_{i,s}$ is the surface temperature at different locations, T_i the corresponding thermocouple reading, K_{cu} the thermal conductivity of the copper block (391 W/m^oK), t the distance between thermocouple position and top surface (2.5 mm), and A_t heat transfer area.

Average surface temperature and effective heat flux have been calculated using:

$$T_s = (T_{1,s} + T_{2,s} \dots + T_{n,s})/n \quad (3.5)$$

$$q_{eff} = Q/A_t \quad (3.6)$$

The average heat transfer coefficient has been calculated using:

$$h_{sp} = q_{eff}/(T_s - T_m) \quad (3.7)$$

3.6. EXPERIMENTAL UNCERTAINTIES

The thermocouples have been calibrated by using a water bath and estimated uncertainty has been ± 0.5 °C. The uncertainty of the water flow measurement has been determined as ± 0.1 %. The accuracy of the power supply has been estimated as ± 2 %.

The uncertainty of a calculated parameter has been obtained based upon the uncertainty in measured variables using the following equation [26] :

$$U_p = \sqrt{\left(\sum_{i=1}^n \frac{\partial p}{\partial a_i} u_{a_i} \right)^2}$$

Where, U_p is the uncertainty in calculating parameter p , a_i is the variables of functional dependence and u_{a_i} is the uncertainty associated with the measurement of each a_i . Using this formula the uncertainties in different calculated parameters are shown in Table 3.1.

Table 3.1: uncertainty associated with the experiment

Parameter	Uncertainty
D_h	3 %
Re	5 %
q	6 %
h	11 %
Nu	12 %
X^*	5 %

CHAPTER 4

NUMERICAL MODEL AND SIMULATION METHODS

In this chapter, three-dimensional fluid flow and heat transfer characteristics have been studied numerically using the commercial computational fluid dynamics (CFD) package FLUENT. The experimental results presented in the previous chapter are used to verify the model. Then some parametric studies are performed by using this model.

4.1. SCHEMATICS OF THE MODEL

The halves of the actual configurations with seven channels, one heater as shown in Figure 5.1. Three cases have been chosen for numerical analysis. Due to symmetry the results have been extended for the entire heat sink. Within the heat sink a conjugate heat transfer occurs combining heat conduction within the solid region and heat convection to the cooling liquid

The key dimensions are also illustrated in the table 4.1. The computational domain is mainly consists of two rectangular channels, and two interconnects. The cross section of the model configuration is presented in Figure 4.1 (b). For the rectangular cross flow four configurations are introduced as shown in Figure 4.1 (c) .

Table 4.1: Key dimensions of the model

Channel	50mm× 5mm (length ×height)
Wall	50mm×5mm (length ×height)
Interconnector	2mm×5mm (length ×height)

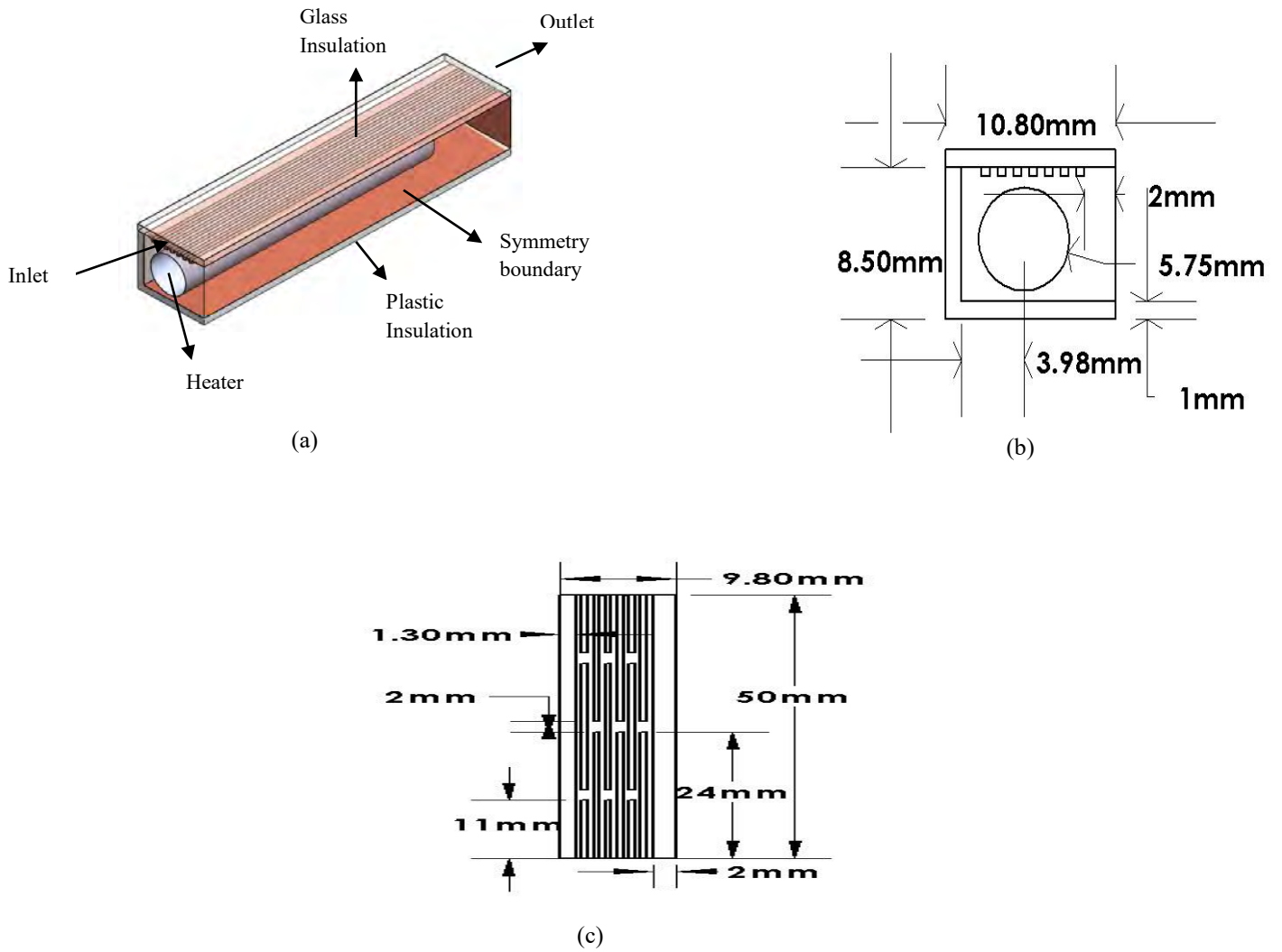


Figure 4.1: Computational domain (a) Simple micro-channel (b) Cross section of computational domain (c) Transverse channels

4.2. MATHEMATICAL FORMULATION

Several assumptions have been incorporated before establishing governing equations for the fluid flow and heat transfer in the minichannel and interconnector:

- (1) Incompressible fluid.
- (2) Laminar flow in the minichannel.
- (3) Negligible radiation and natural convection heat transfer from the minichannel heat sink.
- (4) Negligible axial conduction.
- (5) Constant fluid properties.

In assumption (5), the liquid properties are assumed constant because variations of these properties are small within the temperature range tested.

The incompressible governing equations used to describe the fluid flow and heat transfer in the system is expressed as follows. The conservation equations consist of :

Continuity equation:

$$\nabla \cdot V = 0 \quad (4.1)$$

Navier-Stokes equation:

$$\rho \frac{\partial V}{\partial t} + \rho V \cdot \nabla V = -\nabla P + \nabla \cdot \mu \nabla V \quad (4.2)$$

Energy equation:

$$\rho C_p \frac{\partial T}{\partial t} + \rho C_p V \cdot \nabla T = k \nabla^2 T \quad (4.3)$$

The overall thermal resistance can be defined by-

$$R_t = \frac{T_{w,max} - T_{i,f}}{q} \quad (4.4)$$

The pumping power required to drive the coolant through the mini channel is given by

$$PP = (P_{in} - P_{out}) \times Q \quad (4.5)$$

The local Nusselt number is calculated using the following equation

$$Nu_x = \frac{h_x D_h}{k} \quad (4.6)$$

The local heat transfer coefficient is calculated using

$$h_x = \frac{q}{T_{x,w} - T_{e,f}} \quad (4.7)$$

4.3. BOUNDARY CONDITIONS

4.3.1. Hydraulic Boundary Conditions

First, consider the hydraulic boundary conditions. A uniform velocity is applied at the channel inlet. Thus,

$$u = u_{in}, v = 0, w = 0$$

A pressure outlet boundary condition is specified at the channel outlet. Pressure outlet boundary conditions require the specification of a static (gauge) pressure at the outlet boundary. The pressure at the channel outlet has been considered as atmospheric. The ‘No Slip’ boundary condition at the wall has been applied for solving momentum equations.

4.3.2. Thermal Boundary Conditions

The inlet velocity varied from 0.24m/s to 2.38m/s. The inlet temperature of the cooling water has been set to a constant value at the channel inlet. Thus, over the entire inlet surface, it is assumed:

$$T = T_{in}$$

A constant temperature of 298.1 K has been applied at the channel inlet and the simulation has been completed for two heat generation rate of 6356540 w/m^3 and 13316529 w/m^3 has been applied to the heater volume corresponding to 2.57 w/m^2 and 5.04 w/m^2 .

The natural convection heat transfer from the surfaces of the minichannel heat sink to the atmosphere for both cases has been considered as negligible.

4.3.3. Coolant and Material property of the heat sink

The coolant for both the model has been water and the heat sink material has been copper. The property of the coolant and heat sink material has been considered as constant. The property of different material used in this simulation is presented in the table below:

Table 4.2: The Material property used in the simulation

Material	Density,(kg/m^3)	Specific heat, C_p (j/kg-k)	Thermal Conductivity,k (w/m-k)
Copper	8978	381	387.6
Glass	2700	840	0.0025
Plastic	1150	1670	0.2
Water	996.2	4182	0.6

The viscosity of water has been considered as a linear function of temperature and all other properties Have been considered constant.

4.4.SIMULATION SETUP

The governing equations together with the boundary conditions have been solved using the finite-volume based computational fluid dynamics (CFD) software package, FLUENT 6.3. The laminar model has been employed to compute the flow field. A segregated solution method has been used as the numerical scheme. The first order implicit scheme has been selected for steady formulation. The first order upwind schemes have been employed for momentum and energy equations. The SIMPLE algorithm has been used for pressure-velocity coupling. With these imposed conditions, the steady, incompressible Navier-Stokes equations within the computational domain have been solved along with the energy equation for the specific operating conditions. Convergence criterion has been set for the computation as 10^{-6} .

4.5.MESH INDEPENDENCE TEST

Governing equations have been solved using the laminar model as the maximum Reynolds number under consideration has been 96.91. The computational model has been verified using grid independence test. Two different sizes of uniform mesh have been generated for a single minichannel. The center line temperature of the minichannel for two different sizes of mesh has been compared (total mesh 115000 and 242223). The difference in result for these two sizes of mesh has been less than 0.06%. Therefore, 115000 meshes Have been considered adequate and this grid spacing has been used for all the cases run in this study.

CHAPTER 5

RESULTS AND DISCUSSION

This chapter presents the results of experimental and numerical study of the test section module as presented in the previous section. In the first section of this chapter, experimental results of the thermal performance of the minichannel heat sink are presented followed by the results of the numerical investigation.

5.1. RESULTS OF THE EXPERIMENTAL STUDY

5.1.1. BENCHMARK TEST

Prior to testing the heat sink with cross channel, the heat sink consisting of straight minichannel have been investigated to validate the experimental setup. The heat transfer coefficients in terms of average Nusselt number have been calculated and compared with the previous published results. Figure 5.1 shows the average Nusselt number versus Reynolds number of the channel flow. The test results have been compared with the test result of the fang's experiment [12].

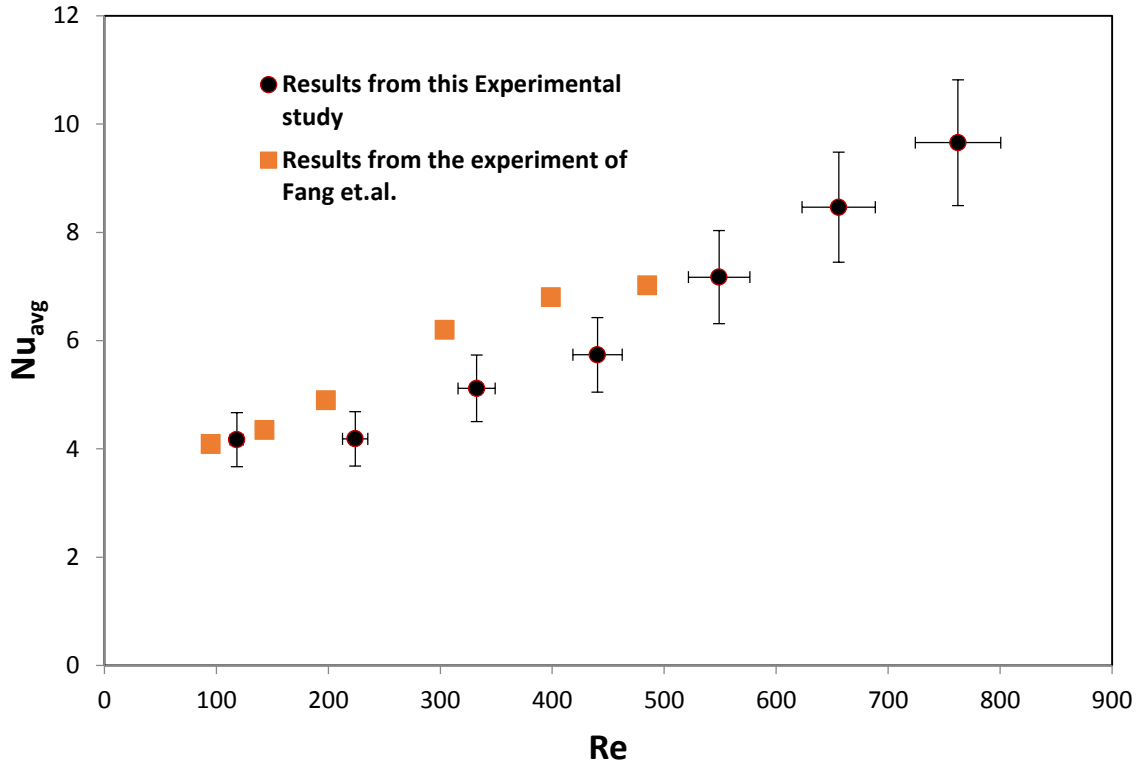


Figure 5.1: Nusselt number as a function Reynolds number

The test results agreed well with the experimental results, however the test assembly of the current study was a little different than that of the fang’s experiment. The test section was 5 mm extended than that of the cartridge heater whereas fang’s test section and the cartridge heater has been of the same length.

Hydrodynamic and Thermal developing length of the test cases have been calculated as presented in the table below:

Table 5.1.1: Entry length for the test cases

<i>Re</i>		112	218	326	434	543	651	758
Hydrodynamic entry length ($L_{\text{entry}} = 0.06D_h Re$)	mm	2.8	5.4	8.1	10.1	13.5	16.2	18.9
Thermal entry length ($L_{\text{entry}} = 0.06D_h Re Pr$)	mm	19.6	38.1	57.1	75.9	95.0	113.9	132.6

As can be seen from the above table, the hydrodynamic developing length covers a large portion of the channel and for Reynolds number more than 300, the thermal entrance length is more than the channel length. As a result, heat transfer has been more compared to the Nu 3.61 for fully developed channel flow.

5.1.2. PERFORMANCE OF THE HEAT SINK

The temperature distribution along the length for the sink at different Re is displayed in Figure 5.2. As already mentioned in the previous section, the thermocouples are located 2.5 mm below from the top surface of the heat sink. The locations, as measured from the inlet of the microchannel and along its length are 5 mm, 15 mm, 25 mm, 35 mm, 45 mm. From the thermocouple readings, it is apparent that the temperature along the length of heat sink increases slightly as we move from upstream to the downstream for all test cases. The maximum standard deviation in temperature measurement is less than 1% at the highest Re. In all cases, the heat input to the cartridge heater has been maintained at ~ 31 Watts. As the heat sink has been elongated by 5 mm from the cartridge heater, temperature of the thermocouple located at the end has been observed to decrease. Heat sink temperature has been observed to decrease at the end of the thermocouple.

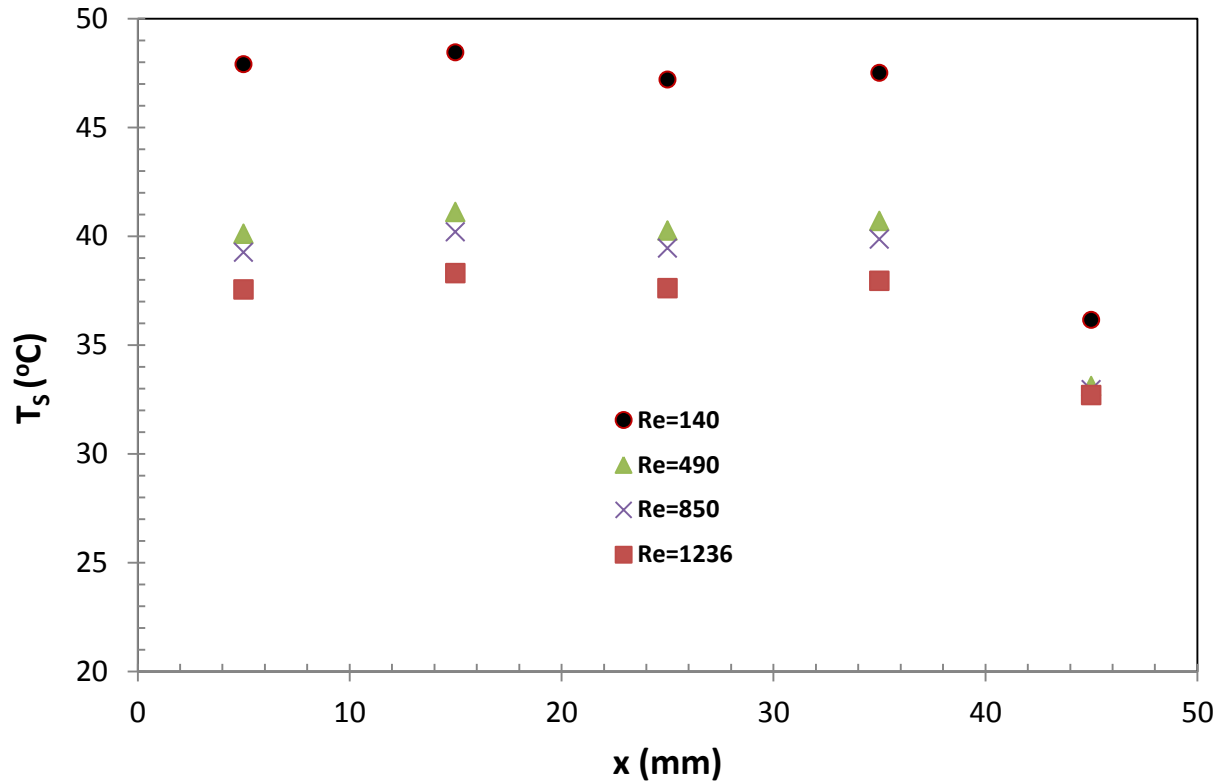


Figure 5.2: Copper heat sink temperature at different thermocouple location and different Reynolds no.

Figure 5.3 shows the comparison of copper heat sink temperature at Reynolds number ~ 150 with that of the heat sink having cross connection. In both the cases, the Power input to the cartridge heater has been maintained at ~ 31 Watts. From the curves, it can be clearly observed that the channel with cross connection heat sink temperature is lower compared to that of the classical minichannel heat sink. These results also confirm the superior thermal performance of the heat sink having cross connection. Similar curves have been obtained for each Reynold's number tested.

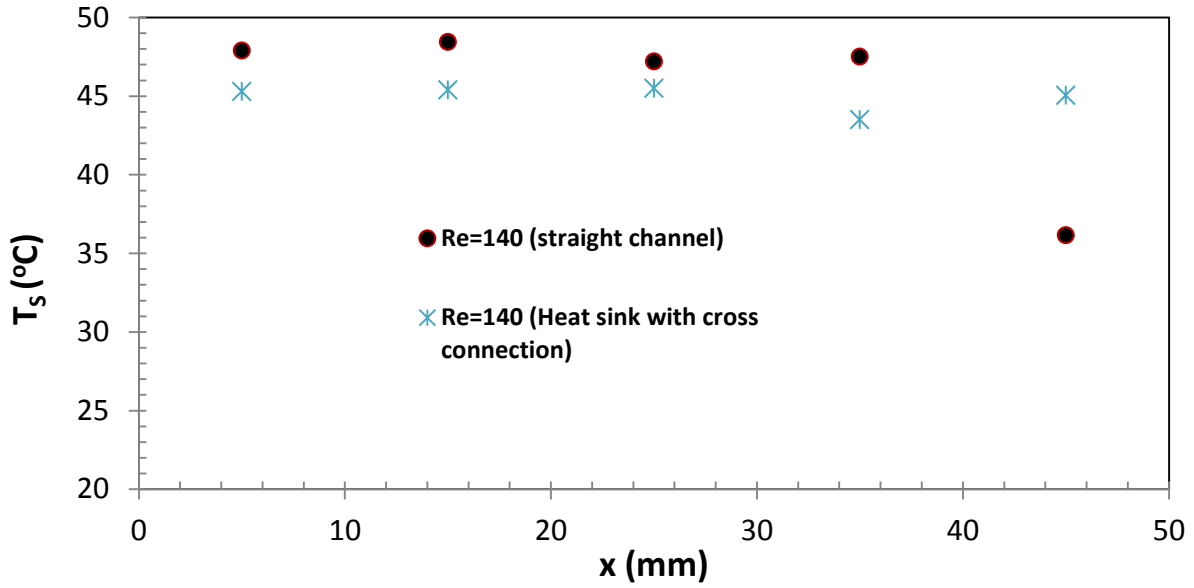


Figure 5.3: Comparison of the Surface temperature between the channel having cross connection and does not have any cross connection.

The test has been conducted at two different input power and as expected surface temperature has been high for the higher input Power. Figure 5.4 presents the surface temperature of the heat sink without cross channel for different Reynol's number.

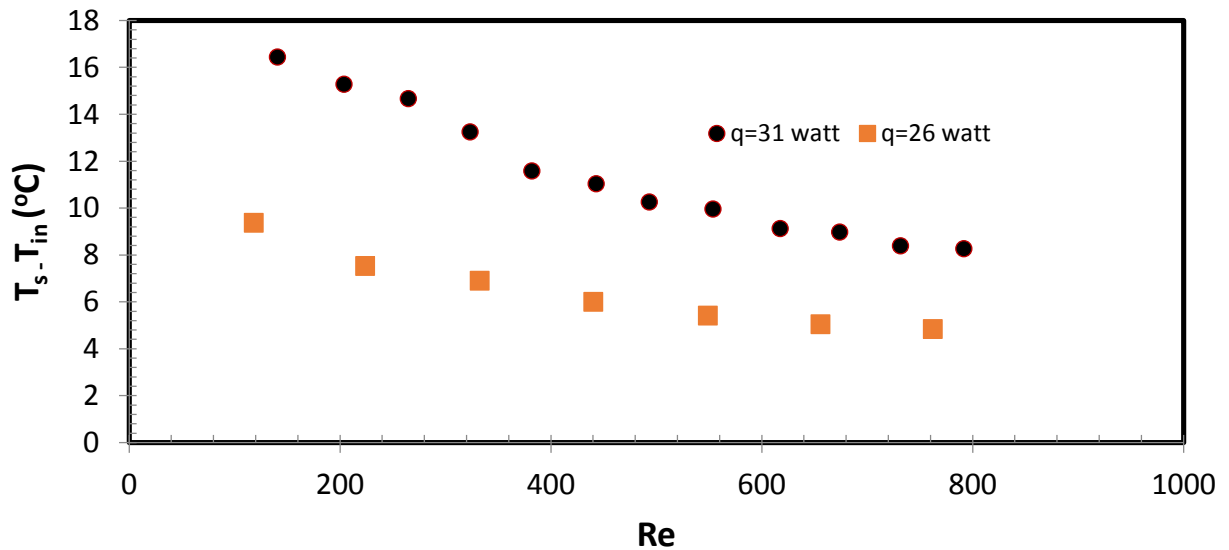


Figure 5.4: Comparison of the Surface temperature for different input power.

However, the input power has little influence on the overall heat transfer coefficient. The average heat transfer coefficient for both the input power shows similar behavior.

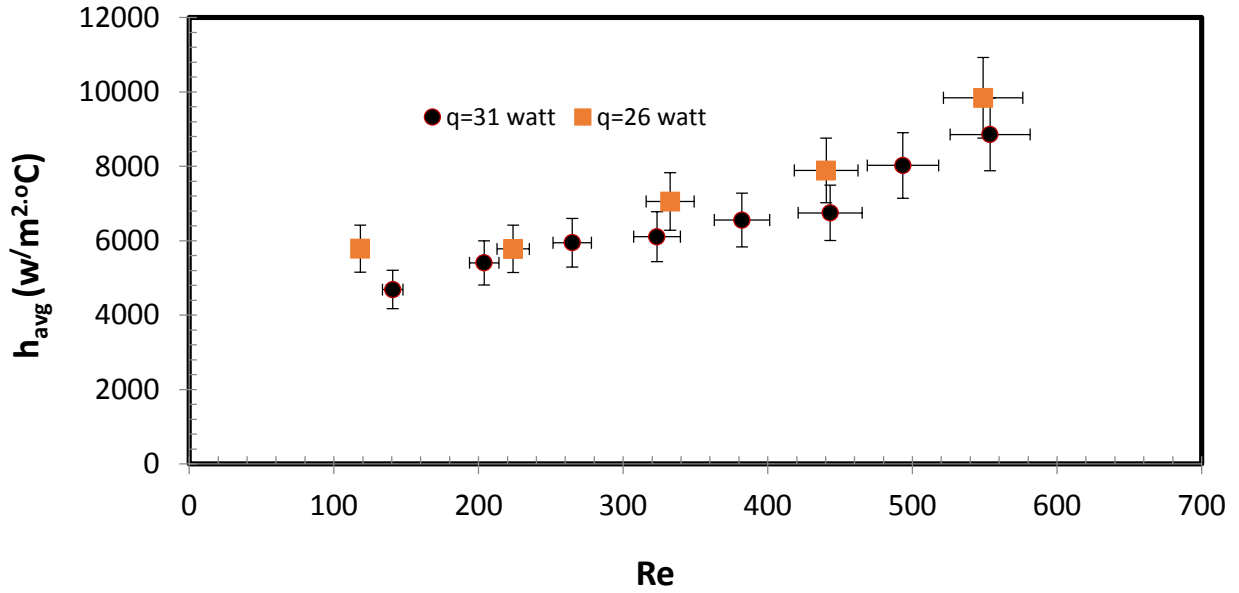


Figure 5.5: Comparison of the average heat transfer coefficient for different input power.

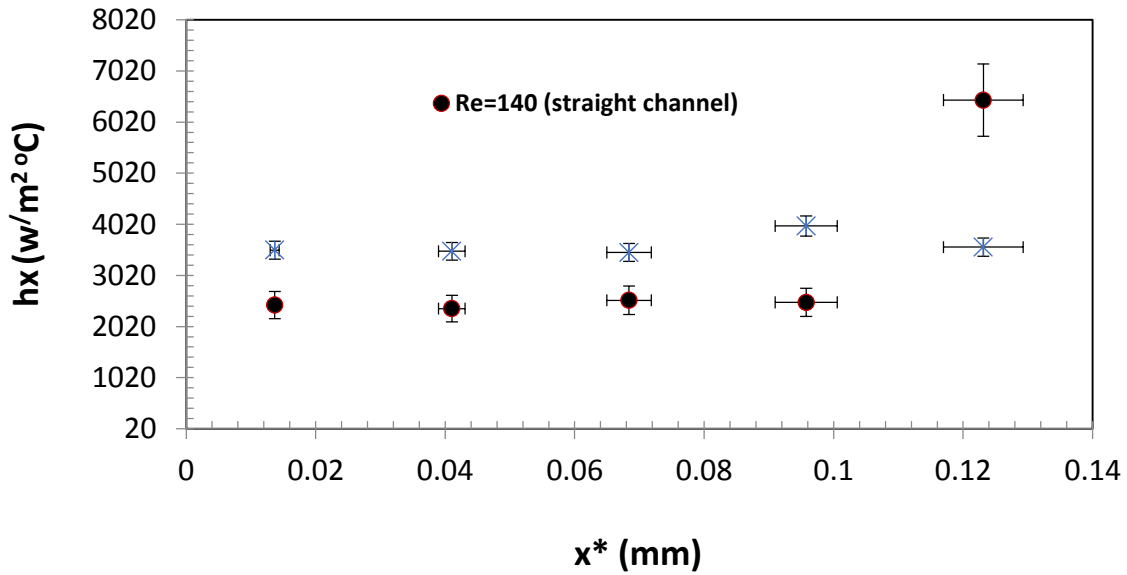


Figure 5.6: Comparison of the h_x as a function of x^* for both the straight channel heat sink and heat sink with cross connection

The comparison of the local heat transfer coefficient as a function of non dimensional length x^* is presented in the Figure 5.6. The Figure 5.6 is plotted for the Reynold's no. 150. Around 10% enhancement in heat transfer coefficient has been observed for the channel having cross connection.

The comparison of average Nu as a function of Re between the straight channel and the channel with the cross connection has been presented in the Figure 5.7. Due to a break up in the continuous flow of the channel of the cross connection, the boundary layer of the fluid breaks up and a new boundary layer grows. Heat transfer coefficient of the boundary layer reduces as it grows. As the boundary layer redevelops in the cross connection, local heat transfer coefficient increases, which increase the overall heat transfer coefficient. About 18% enhancement has been observed for the cross connection compared to the channel without cross connection.

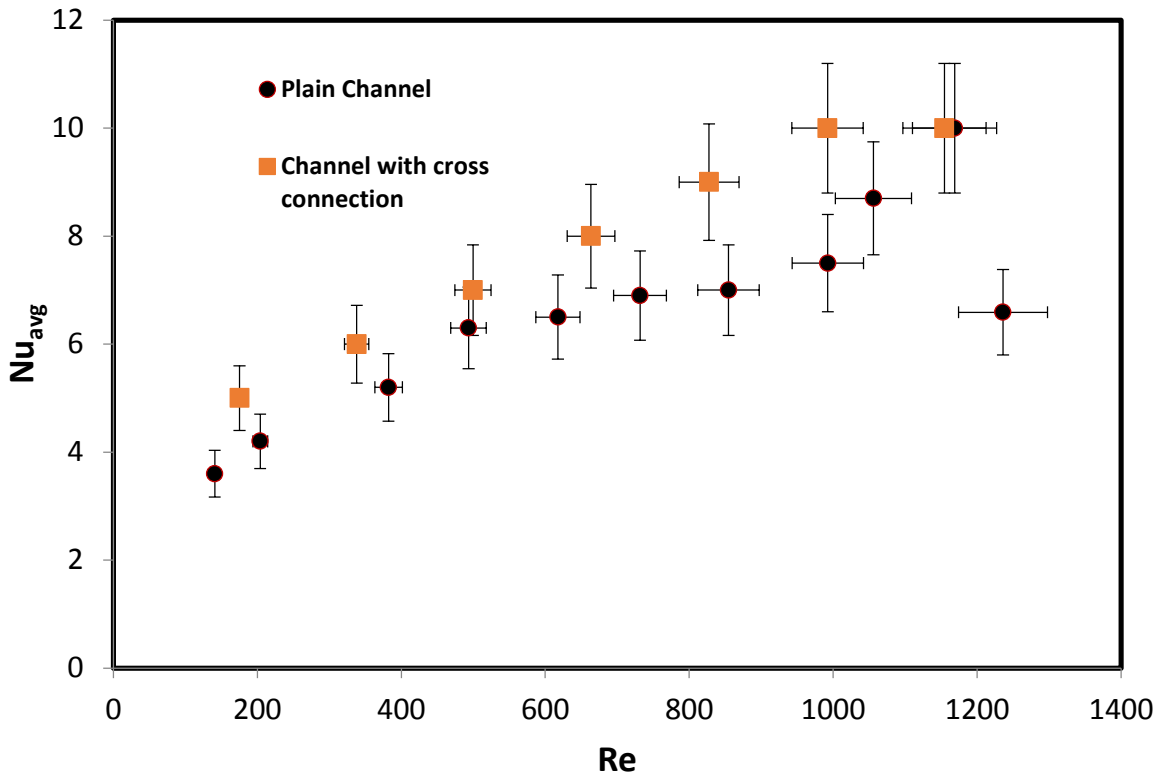


Figure 5.7: Comparison of the Nu_{avg} as a function of Re for both the straight channel heat sink and heat sink with cross connection

5.2.RESULTS OF THE NUMERICAL STUDY

5.2.1. MODEL VALIDATION

Figure 5.8 presents the comparison between the experimental and simulation results. Applied input power has been ~ 27 watt corresponding to 15870 w/m^2 heat flux. Average Nusselt no. obtained from the simulation for different Reynold's no. is very much comparable and the deviation between the experimental and simulation results Have been computed as 8.5% at the Reynold's no. of 720 and 16% at the Reynold's No. of 820.

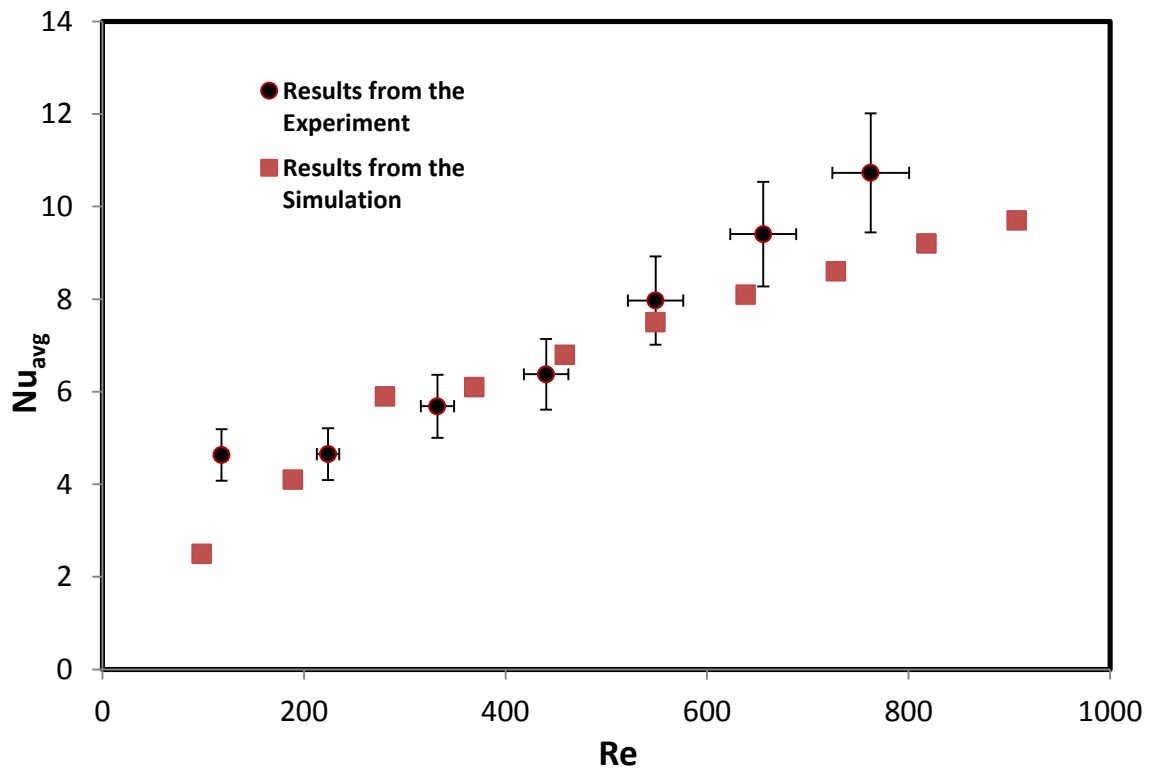


Figure 5.8: Comparison of the experimental results with that of the simulation for straight mini channel

5.2.2. EFFECT OF THE CHANNEL ENLARGEMENT

One of the major challenges of minichannel heat sink is the temperature gradient along the flow direction. If the channel carrying the coolant is extended than the length of the heating zone, temperature gradient along the length significantly drops as the heat from the source gets more substrate space to dissipate. Figure 5.9 compares the results of the numerical simulation between the heat sink having elongated channel and channel have the same length as that of the heat source.

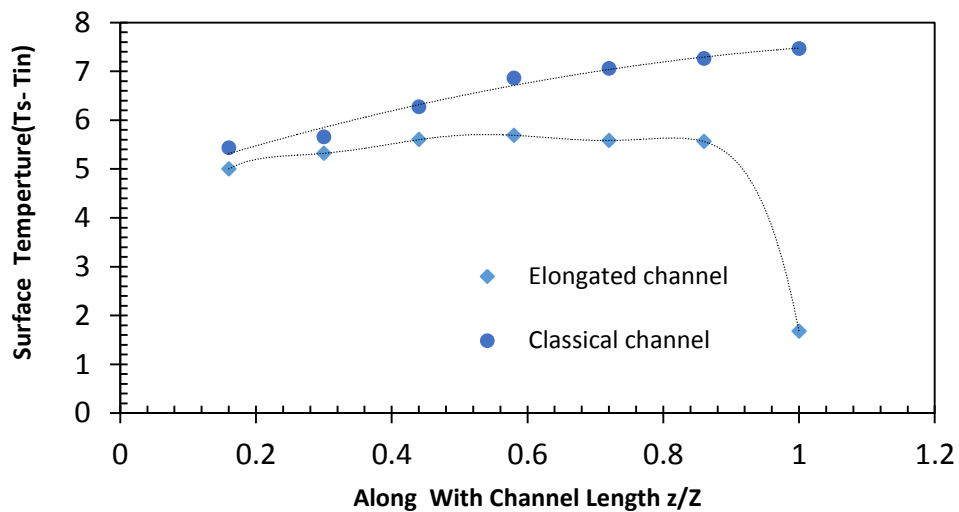


Figure 5.9: Comparison of the experimental results with that of the simulation for straight mini channel

The formation of velocity and thermal boundary layer within the mini channel reduces local heat transfer, which increase the local surface temperature. Along the channel length the surface temperature increases, but since the cartridge heater was not extended up to the channel outlet the temperature fall in that region. The Figure 5.10 shows the 3-D plot of temperature contour for simple micro-channel computational domain for $q_1=13.5$ Watt and at $Re=98$.

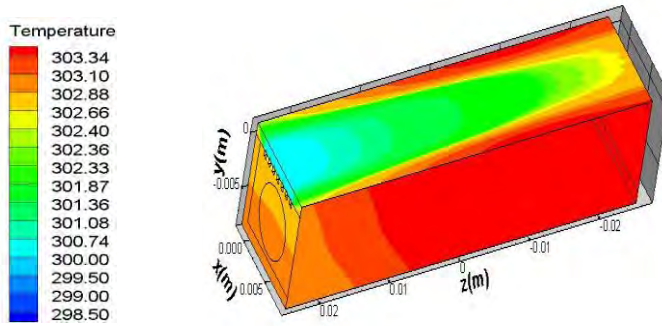


Figure 5.10: plot of temperature contour for simple micro-channel computational domain for $Re=98$

5.3.EFFECT OF THE FLOW VELOCITY

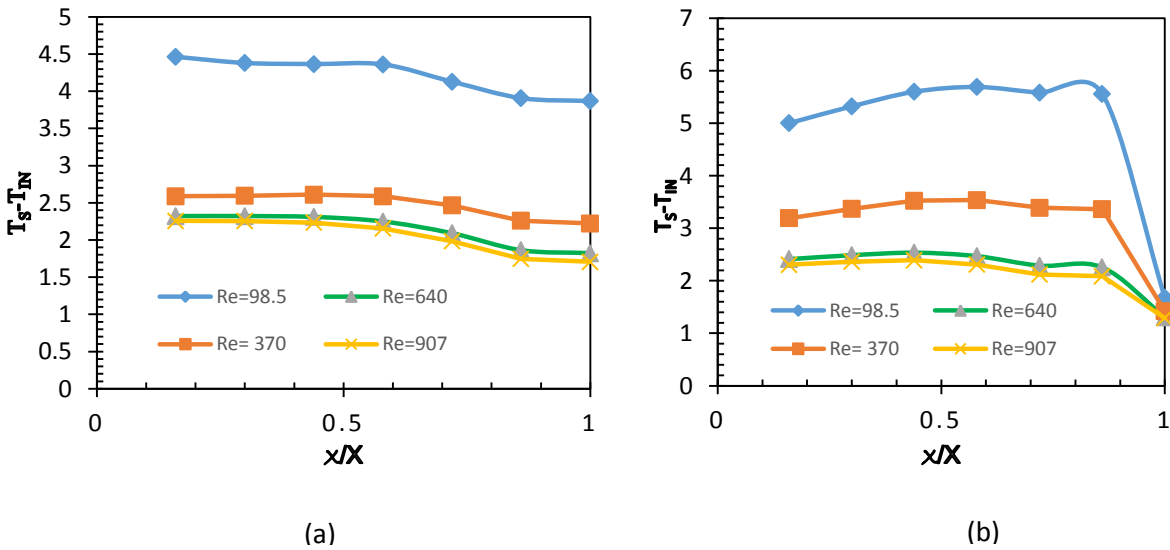


Figure 5.11: Effect of the velocity on the temperature distribution of the channel (a) heat sink with the cross channel; (b) heat sink without cross channel

With the increase of velocity heat transfer rate in the mini channel heat sink increase in all the cases. Figure 5.11 presents surface temperature rise compared to the inlet water temperature for both the heat sink with cross connection and without cross connection. Due to better heat transfer in the heat sink to cross connection, temperature is more uniform than that of the mini channel heat sink without interconnections. To understand the insight phenomena contour of the channel is investigated as presented in the Figure 5.12.

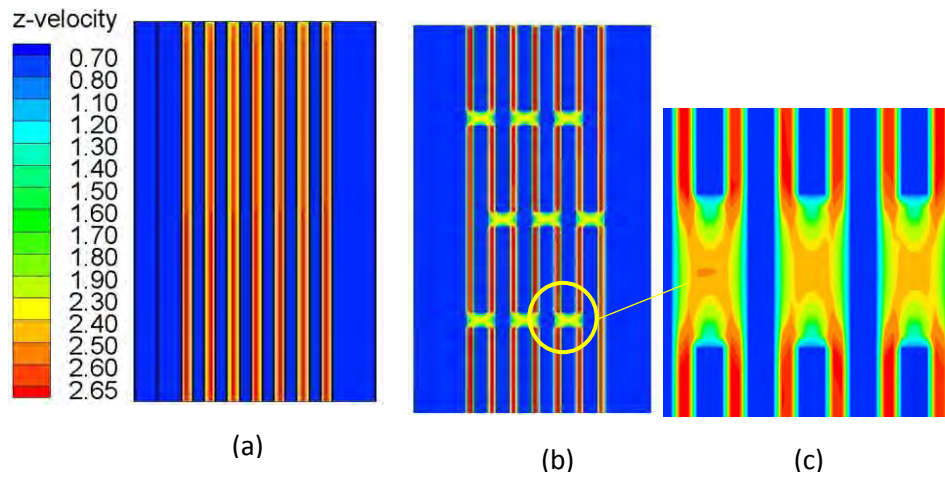


Figure 5.12: Velocity contour of the heat sink (a) channel without cross connection; (b) channel with cross connection; (c) boundary layer redevelopment around the cross connection

As evident from Figure 5.12 (c), boundary layer at the cross connection brakes up and a new boundary layer redevelops which causes the enhancement in heat transfer rate for the cross connected channel.

5.3.1. EFFECT OF THE CROSS CONNECTION

The interconnects are flow path for the coolant, which allows the coolant to flow between the channels. It has been demonstrated that the interconnections can reduce thermal resistance. To investigate the effect of interconnections on the overall heat transfer performance of the mini channel interconnected heat sink, the simulations have been conducted as presented in the Figure 5.13.

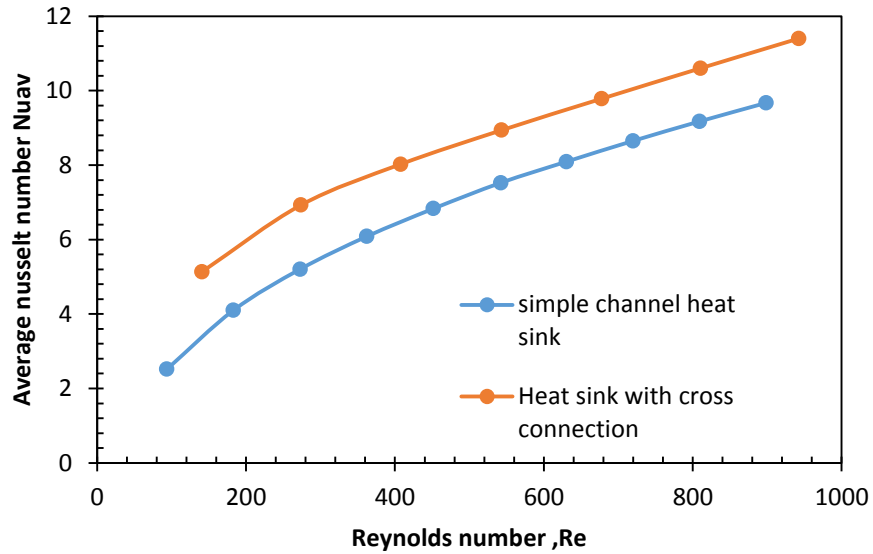


Figure 5.13: Average Nusselt number as a function of the Reynolds number

Figure 5.13 compares the numerical result of the straight channel heat sink and compares with that of the minichannel heat sink with cross connections. Around 18% enhancement in average Nusselt number has been observed for the minichannel heat sink with cross connections. To get the insight of this enhancement, the temperature contour of the mini channel has been analyzed as presented in the Figure 5.14.

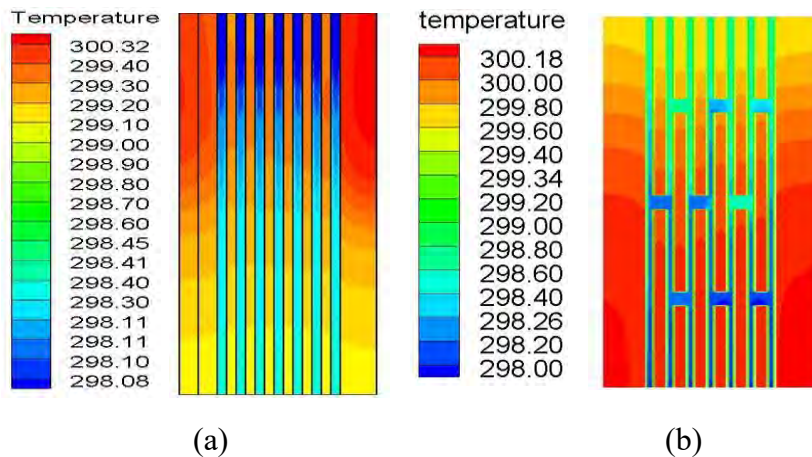


Figure 5.14: Temperature contour of heat sink at the plane at $y=0$ for 76 volt and $Q=500\text{ml/min}$
 (a) simple micro-channel (b) transverse micro-channel

The minichannel configuration with cross channel introduces disruption in the thermal and velocity boundary layer via cross flow and local turbulence generation which causes the increase in heat transfer rate of this configuration.

The pumping power requirement is also a very significant term for designing heat sink. High pumping power corresponds to a higher pressure penalty which can offset the heat transfer enhancement. Figure 5.15 compares the overall thermal resistance for the two configurations of the heat sink with pumping power. Increase of pumping power by introducing transverse mini - channel offsets the overall thermal resistance. The overall thermal resistance decreases with the pumping power. For the same pumping power around 40% decrease in thermal resistance has been observed for the minichannel with cross connection.

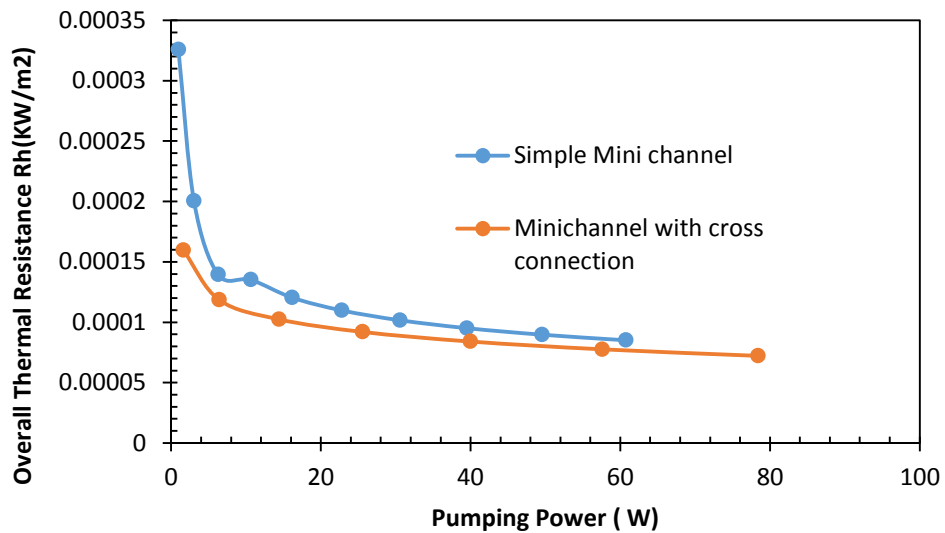


Figure5.15: Overall thermal resistance vs pumping power

CHAPTER -6

CONCLUSION AND FUTURE RECOMMENDATION

6.1.CONCLUSIONS

From the study of this research, following conclusion may be drawn:

1. Zoning the minichannel with the cross cut is effective in enhancing its heat transfer performance. Around 18% enhancement in heat transfer performance has been achieved in this experiment for the minichannel heat sink having the cross connection compared with that of the straight minichannel heat sink.
2. Temperature gradient along the flow path becomes less gradient for the minichannel heat sink with cross connection.
3. Enlargement of the channel section compared to the heating surface is also effective in reducing the temperature gradient along the channel length.
4. Good agreement has been achieved between the experimental data and numerical predictions for the averaged Nusselt number of the heat sink.
5. The three-dimensional steady laminar model may be used to predict the heat transfer characteristics of minichannel flow with with cross connection.
6. Input heat fluxes within the limiting range has no effect on the overall thermal performance of the mini channel heat sink.
7. For the same pumping power cross connected minichannel may reduce thermal resistance by 40%.

6.2.FUTURE RECOMMENDATIONS

1. In this study, heat transfer performance of the heat sink with cross connection has been studied up to Reynold no 1000. The study may be further extended for higher Reynold number.
2. The experimental work may be carried out for two phase flow condition to understand the effect of the cross connection on two phase flow.
3. Instead of minichannel, microchannel heat sink may be considered for further analysis.
4. More extensive numerical work can be carried out for the minichannel heat sink with wall jet.

REFERENCES

- [1] A. Bar-Cohen, P. Wang, and E. Rahim, "Thermal management of high heat flux nanoelectronic chips," *Microgravity Science and Technology*, vol. 19, no. 3, pp. 48-52, 2007.
- [2] S. Kandlikar, S. Garimella, D. Li *et al.*, *Heat transfer and fluid flow in minichannels and microchannels*: elsevier, 2005.
- [3] R. S. Prasher, J. Y. Chang, I. Sauciu *et al.*, "Nano and Micro Technology-Based Next-Generation Package-Level Cooling Solutions," *Intel Technology Journal*, vol. 9, no. 4, pp. 285-296, 2005.
- [4] R. Fang, W. Jiang, J. Khan *et al.*, "Experimental Heat Transfer Enhancement in Single-phase Liquid Microchannel Cooling With Cross-flow Synthetic Jet." pp. 681-689.
- [5] C. J. Lasance, and R. E. Simons, "Advances in high-performance cooling for electronics," *Electronics Cooling*, vol. 11, no. 4, 2005.
- [6] S. V. Garimella, and C. B. Sobhan, "Transport in microchannels-a critical review," *Annual review of heat transfer*, vol. 13, no. 13, 2003.
- [7] D. B. Tuckerman, and R. Pease, "High-performance heat sinking for VLSI," *IEEE Electron device letters*, vol. 2, no. 5, pp. 126-129, 1981.
- [8] E. G. Colgan, B. Furman, M. Gaynes *et al.*, "A Practical Implementation of Silicon Microchannel Coolers for High Power Chips," *IEEE Transactions on Components and Packaging Technologies*, vol. 30, no. 2, pp. 218 - 225, 2007.
- [9] M. E. Steinke, and S. G. Kandlikar, "Review of single-phase heat transfer enhancement techniques for application in microchannels, minichannels and microdevices," *International Journal of Heat and Technology*, vol. 22, no. 2, pp. 3-11, 2004.
- [10] J. S. Go, "Design of a microfin array heat sink using flow-induced vibration to enhance the heat transfer in the laminar flow regime," *Sensors and Actuators A: physical*, vol. 105, no. 2, pp. 201-210, 2003.
- [11] M.-A. Hessami, A. Berryman, and P. Bandopdhayay, "Heat transfer enhancement in an electrically heated horizontal pipe due to flow pulsation." pp. 49-56.
- [12] R. Fang, W. Jiang, J. Khan *et al.*, "Experimental Heat Transfer Enhancement in Single-Phase Liquid Microchannel Cooling With Cross-Flow Synthetic Jet," no. 49408, pp. 681-689, 2010.
- [13] J. A. Khan, A. K. M. M. Morshed, and R. Fang, "Towards Ultra-compact High Heat Flux Microchannel Heat Sink," *Procedia Engineering*, vol. 90, no. Supplement C, pp. 11-24, 2014/01/01/, 2014.
- [14] M. K. Sung, and I. Mudawar, "Single-phase hybrid micro-channel/micro-jet impingement cooling," *International Journal of Heat and Mass Transfer*, vol. 51, no. 17, pp. 4342-4352, 2008.
- [15] A. K. M. M. Morshed, F. Yang, M. Yakut Ali *et al.*, "Enhanced flow boiling in a microchannel with integration of nanowires," *Applied Thermal Engineering*, vol. 32, no. Supplement C, pp. 68-75, 2012/01/01/, 2012.
- [16] Y. Peles, A. Koşar, C. Mishra *et al.*, "Forced convective heat transfer across a pin fin micro heat sink," *International Journal of Heat and Mass Transfer*, vol. 48, no. 17, pp. 3615-3627, 2005/08/01/, 2005.
- [17] J. L. Xu, Y. H. Gan, D. C. Zhang *et al.*, "Microscale heat transfer enhancement using thermal boundary layer redeveloping concept," *International Journal of Heat and Mass Transfer*, vol. 48, no. 9, pp. 1662-1674, 2005/04/01/, 2005.
- [18] Y. Xuan, and Q. Li, "Heat transfer enhancement of nanofluids," *International Journal of Heat and Fluid Flow*, vol. 21, no. 1, pp. 58-64, 2000/02/01/, 2000.

- [19] B. C. Pak, and Y. I. Cho, "HYDRODYNAMIC AND HEAT TRANSFER STUDY OF DISPERSED FLUIDS WITH SUBMICRON METALLIC OXIDE PARTICLES," *Experimental Heat Transfer*, vol. 11, no. 2, pp. 151-170, 1998/04/01, 1998.
- [20] U. Rea, T. McKrell, L.-w. Hu *et al.*, "Laminar convective heat transfer and viscous pressure loss of alumina–water and zirconia–water nanofluids," *International Journal of Heat and Mass Transfer*, vol. 52, no. 7, pp. 2042-2048, 2009/03/01/, 2009.
- [21] V. Bianco, F. Chiacchio, O. Manca *et al.*, "Numerical investigation of nanofluids forced convection in circular tubes," *Applied Thermal Engineering*, vol. 29, no. 17, pp. 3632-3642, 2009/12/01/, 2009.
- [22] C. H. Chon, K. D. Kihm, S. P. Lee *et al.*, "Empirical correlation finding the role of temperature and particle size for nanofluid (Al₂O₃) thermal conductivity enhancement," *Applied Physics Letters*, vol. 87, no. 15, pp. 153107, 2005/10/10, 2005.
- [23] J. C. Sturgis, and I. Mudawar, "Single-phase heat transfer enhancement in a curved, rectangular channel subjected to concave heating," *International Journal of Heat and Mass Transfer*, vol. 42, no. 7, pp. 1255-1272, 1999/04/01/, 1999.
- [24] C.-P. Jen, C.-Y. Wu, Y.-C. Lin *et al.*, "Design and simulation of the micromixer with chaotic advection in twisted microchannels," *Lab on a Chip*, vol. 3, no. 2, pp. 77-81, 2003.
- [25] F. Bondar, and F. Battaglia, "A Computational Study on Mixing of Two-Phase Flow in Microchannels," no. 37165, pp. 101-109, 2003.
- [26] S.-Y. Cho, and C. Park, "a study on the propagation of measurement uncertainties into the result on a turbine performance test," *KSME International Journal*, vol. 18, no. 4, pp. 689-698, April 01, 2004.